ACS Medicinal Chemistry Letters

Letter

pubs.acs.org/acsmedchemlett

Peptidic Inhibitors for in Vitro Pentamer Formation of Human Papillomavirus Capsid Protein L1

Ding-Yi Fu,[†] Shi Jin,[†] Dong-Dong Zheng,[†] Xiao Zha,[‡] and Yuqing Wu*[,†]

[†]State Key Laboratory of Supramolecular Structure and Materials, Institute of Theoretical Chemistry, Jilin University, No. 2699, Qianjin Street, Changchun 130012, China

[‡]Sichuan Tumor Hospital & Institute, Chengdu 610041, China

Supporting Information

ABSTRACT: A new 14 peptide, originating essentially from the helix 5 of HPV 16L1, illustrates an IC_{50} of 19.38 nM for the inhibition of HPV 16 L1 pentamer formation, which is highly efficient for targeting a specific protein segment. In addition, mechanism studies reveal that the length, sequence, and the folding of the peptide are critical factors for its inhibition. Particularly, the peptide shows similar inhibition against the pentamer formation of HPV 58L1, although it is designed specially for HPV 16 L1. This study opens a way for the development of high-efficiency, broad-spectrum inhibitors as a new class of anti-HPV agents, which could be extended to the treatment of other virus types.

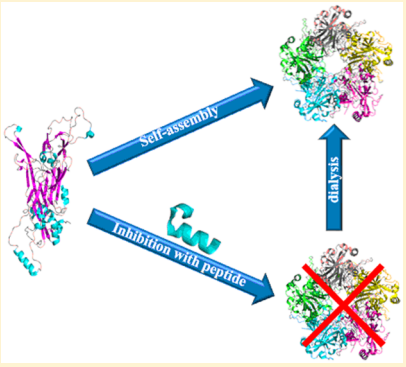

KEYWORDS: *Peptide, inhibitor, pentamer formation, human papillomavirus*

Human papillomaviruses are known etiologic causes of cervical cancer in women.[1−4] The major capsid protein L1 and minor capsid protein L2 are constructs of the virus particles that are essential for the mediation of the primary attachment of viral particles to cells[5] and the extracellular matrix,[6] and are therefore required for viral infections.[7−10] Current PV vaccines have shown effective protection against infection with a limited number of phylogenetically related HPV types, but not against more distantly related subtypes.[11−14] Being type-specific, expensive, and requiring cold storage for transportation, these vaccines have not been widely used in developing countries.[15,16] Therefore, urgent needs exist to develop new agents that are cost-effective and/or provide more broad-spectrum protection. Small organic molecules, short DNA, and/or peptides, designed to target specific protein−protein interactions (PPIs), would be efficient alternative agents because the protein interfaces are formed by multiple, relatively weak noncovalent interactions.[17−23] Cryoelectron microscopic analysis has shown that virion particles consist of 72 capsomeres, and each is a pentamer of the major capsid protein, L1.[24] Large scale investigations have monitored the formation of VLPs from pentamers, few studies have focused on the formation of pentamers,[25−27] although which is the prerequisite for VLPs assembly. Recent efforts to obtain a stable GST-L1 monomer provided a platform to follow the kinetics of L1-p formation,[28] however, specific binding site/segment as an intervention target remains a great challenge. The importance of the helix 5 (h5) near the C-terminus for L1-p formation has been defined by monosite mutation,[29] thereby supplying a possible target for monitoring the pentamer formation by small molecules. Therefore, it is possible to create a synthetic peptide containing h5 of HPV L1 and several amino acids (AAs) before or following it (Table 1) as potential inhibitors of L1-p formation. Incubation of the pep15 with HPV 16 GST-L1 has shown obvious inhibition of the L1-p

Table 1. Sequences and Names of the Synthetic Peptides Based on Helix 5 of HPV 16 L1 (^{462}FPLGRKFLLQAG^{473})

Sequence of peptide	Name
PLGRKFLLQAGLKAK	pep15
DLDQFPLGRKFLLQ	pep14
DLDQFPSSSKFLLQ	pep14LGR-SSS
DLDQFPAGRKFLLQ	pep14L464A
DLDQFPLGAKFLLQ	pep14R466A
DSDQFPLGRKFLLQ	pep14L459S
DLDQSPLGRKFLLQ	pep14F462S
SGFLRQLGFDKLQD	pep14-Scr
DLDQFPLGR	pep9
QFPLGRKFL	pep9′
PLGRKFL	pep7

Received: September 26, 2014
Accepted: February 25, 2015
Published: February 25, 2015

DOI: 10.1021/ml500392y
ACS Med. Chem. Lett. 2015, 6, 381−385

formation in vitro, opening a way for the development of a new class of anti-HPV agents.

In addition, the pentameric crystal structure of truncated HPV 16L1[30] illustrated that h5 was located inside a hydrophobic cavity and was anchored to the central β-barrel core of the subunit via the long side chain of R466 (Figure S1A). In addition, F462 was located in the same hydrophobic region including F468 and H36, where the hydrophobic residue of L459 inserted into the curved surface and formed a hydrophobic chain surrounded by V103. Of special note was that the phenyl ring of F462 in h5 could $\pi-\pi$ stack with the imidazole side chain of H36 (Figure S1B). Furthermore, strong hydrogen bonding was shown between D460 and H319 located in a neighboring subunit; while another hydrogen bond was formed between Q461 and V21 (Figure S1C). Therefore, the sequence of ^{458}DLDQ^{461} located before h5 may be more important than those after it, in keeping the optimum folded structure, and especially to improve its specific binding affinity to L1. We, therefore, designed a new peptide by extending pep15 with five AAs at the N-terminus (pep14, Table 1) instead of at its C-terminus. The characterization of peptide was performed by high-performance liquid chromatography (HPLC) and mass spectrometry (MS) (Figure S1.1).

The inhibition efficiency of pep14 against HPV 16 L1-p formation was detected by using SEC. The GST-L1, either incubated with peptides in advance or not, after overnight digestion by PPase, was injected onto gel-filtration columns and then eluted with a fast protein liquid chromatography (FPLC) procedure (Figure 1). Without pep14 pretreatment, the FPLC

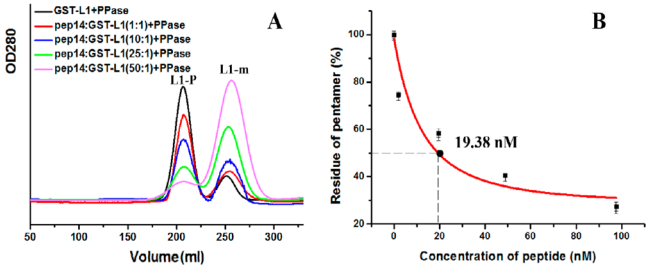

Figure 1. (A) Examinations of the pentamer formation of L1 by SEC. The protein was treated with different molar ratios of pep14 to GST-L1 as indicated. (B) The given curve illustrated the pentamer formation under the inhibition of peptide, showing the IC_{50} response to the peptide.

elution profile showed an intense peak at ~265 kDa, indicative of the HPV L1-p, and a weak peak corresponding to ~53 kDa, which was attributed to the L1-m.[28,29] After GST-L1 was preincubated with different molar ratios of pep14 and following digestion with PPase, the obtained FPLC elution profile exhibited a smaller peak for L1-p and an increased L1-m peak. These changes were illustrated more clearly by the ratio of their integrated peak areas, S_p to S_m, as a function of the pep-14 concentrations (Figure S2). More precisely, the rate of L1-p formation was inhibited by pep14 in a dose-dependent manner, displaying a half concentration (IC_{50}) of inhibition at 19.38 nM for 1.25 nM GST-L1 (Figure 1B). Therefore, the inhibition of L1-p formation by pep14 in vitro was proved to be twice as effective as pep15 (IC_{50} = 48.09 nM) (Figure S3). Thus, the extension of pep15 by five AAs at the N-terminus of h5 was critically important to enhance the inhibitory efficiency.

The potency of pep14 for inhibiting the L1-p assembly in vitro was then investigated by static light scattering (SLS). The GST-L1 monomer could form a pentamer after adding PPase to cleave the GST tag, and the size of the pentamer particle was bigger than the monomer as indicated by dynamic light scattering (DLS) and transmission electron microscopy (TEM). Therefore, pentamer formation led to an increase of the SLS intensity.[28] Such a response could be further used to monitor the interference of the L1-p assembly by pep14. In the absence of pep14, the scattering intensity of the GST-L1 solution increased gradually with time after PPase addition for GST cleavage (Figure 2A), suggesting that the L1 pentamer

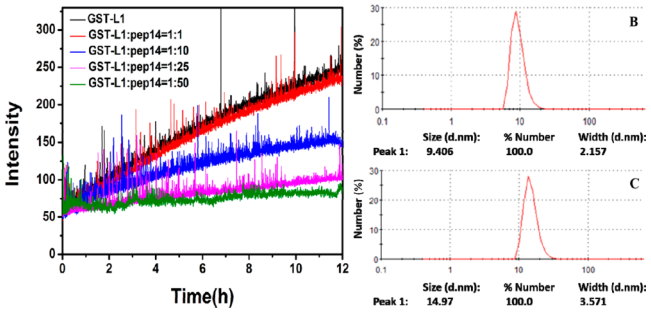

Figure 2. (A) Monitoring of the assembly of pentamers from GST-L1 monomers (1.25 nM) with different concentrations of peptide by time-dependent SLS after addition of the PPase for GST cleavage. The curves in different colors represent the molar ratios of peptide to GST-L1 as indicated, respectively. (B) DLS profiles, showing the hydrodynamic diameter distribution of the protein after incubating with peptide (1:50) and PPase, and (C) that without peptide. The concentration of GST-L1 was 1.25 nM.

formed easily under these conditions. However, in the presence of pep14, the rate was markedly reduced, and the inhibition tendency increased with the addition of more pep14. In the presence of excess pep14 (1:50), the pentamer formation was suppressed almost completely. In addition to excluding the possibility that the intensity of the SLS signal increase was due to protein aggregation, after the above SLS measurement, the solution of GST-L1 was then tested by DLS. The result showed a size distribution of hydrodynamic diameter at ~9.4 nm (Figure 2B), being essentially the L1-m.[29] However, a PPase treated GST-L1 without pep14 showed a size distribution of a hydrodynamic diameter at ~14.9 nm as the size of pentamer (Figure 2C).

Fluorescence resonance energy transfer (FRET) was then performed to confirm the direct binding of pep14 and HPV 16 GST-L1 (Figure 3A). These results illustrated that pep14 could bind tightly to GST-L1, with the protein providing energy as the donor to the nearby acceptor, pep14-CY3. However, the sequence checking of GST showed there were four tryptophans involved as well (Figure S4), which might influence the observed fluorescence data. Therefore, a FRET measurement between pep14-CY3 and pure GST was used to assay the direct binding between GST and pep14. The results (Figure S5A) confirmed that the FRET indeed occurred between L1 and pep14-CY3 and not the GST tag. Furthermore, according to the FRET spectra (Figure 3A), the dissociation constant (K_d) was calculated to be 0.6 ± 0.02 μM (Figure S6).[31]

In addition, under identical conditions, when we used the scrambled pep14, pep14-Scr, instead of pep14, the addition of GST-L1 induced only an emission intensity increase at 340 nm,

DOI: 10.1021/ml500392y
ACS Med. Chem. Lett. 2015, 6, 381−385

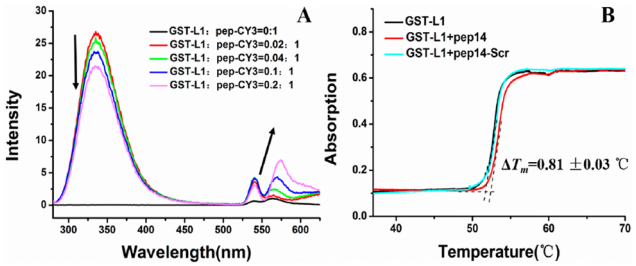

Figure 3. (A) FRET assay between peptide and protein (λ_{ex} = 270 nm). The pep14 was labeled by CY3 in forming pep14-CY3 first, and then the proteins were added to obtain different molar ratios of them. (B) The UV cloud point measurements of HPV 16 GST-L1 (1.25 nM) in mixing with pep14 (1:100) or pep14-Scr (1:100) with temperature ramping (λ = 350 nm). ΔT_m was an average value of three repeat experiments, and each displayed plot was the representative of three.

not at 570 nm (Figure S5B). Thus, the scrambled peptide could not interact with GST-L1, and therefore, we observed no inhibition with it on L1-p formation (Figure S7A). Furthermore, the binding of pep14 and pep14-Scr with GST-L1 was assayed by using UV-cloud point measurements (Figure 3B), where a slightly improved transition temperature (ΔT_m) was obtained for GST-L1 after the addition of pep14 rather than pep14-Scr, indicating specific binding with pep14 and consequent contribution to the thermal stability of the complex.

The GST-L1, after pep14 treatment and following overnight PPase digestion, showed only L1 monomer in this case. Once the mixture was further dialyzed in a large amount of buffer L to remove the peptide and then analyzed by DLS, it showed L1-m could form L1-p again (Figure S8A,B). Furthermore, the solution was dialyzed in assembly buffer, and the particles were then tested by DLS (Figure S8C,D) and TEM (Figure S9). The particle morphology determined by TEM clearly showed the VLPs were almost all of regular size, illustrating that after binding with pep14, the released L1 still had the ability to form VLPs. That is, the inhibition of pep14 on L1 pentamer formation was reversible.

To gain insight into the inhibition mechanism of pep14 toward the L1-p formation, we undertook a structural determination of the peptide by CD spectroscopy.[32] The CD spectrum of pep14 showed a negative band at about 207 nm, together with a positive band at 192 nm (Figure S10A), which is characteristic of an α-helix structure. Therefore, the correct folding of the peptide might be essential for its binding to GST-L1. Furthermore, the mutation and truncation of the peptide were also used to reveal the nature of the binding. The critical importance of ^{464}LGR^{466} in helix 5 for in vitro L1-p formation[29] prompted us to perform the mutation at these three sites first in forming pep14LGR-SSS. Then each site was mutated individually to identify its separate role (Table 1). As expected, none of the mutations caused inhibition of L1-p formation as tested by FPLC (Figure S10B), confirming the critical importance of each site of the peptide in binding with protein. The CD spectrum for pep14LGR-SSS showed a negative peak at 200 nm (Figure S10A) as it existed mainly in a random coil. That is, the mutation damaged the folding of the peptide completely and lead it to lose the ability to bind to the protein, accounting for the loss of inhibition. In contrast, albeit the monosite mutations kept their α-helix structures, they still lost the ability to inhibit L1-p formation. In this case, the folding of the peptide was not important. The previous study showed that the monosite mutations of ^{464}LGR^{466} did not affect the folding of L1 but disrupted the formation of pentamer;[29] being similar here. Therefore, both outcomes were consistent and supported each other well.

To further screen out the critical region of pep14, two truncated shorter peptides, pep9 and pep9′, were then designed and synthesized. To assay the importance of the QF sequence in inhibition, a shorter peptide, pep7, was also synthesized to compare with pep9. The inhibitory potencies of all three peptides on L1-p formation were measured by FPLC and compared (Figure S11A). Of note, the inhibition efficiency of pep9′ was less than that of pep14 but better than that of pep9, although the AA number was the same. However, despite differing from pep9′ by only two AAs, pep7 showed almost no inhibition of L1-p formation. The large inhibition gap between them indicated that the ^{461}QF^{462} in peptides indeed played a key role in the binding to the L1 protein. The ^{461}QF^{462} sequence was located at the start of helix 5, where the F462 residue could $\pi-\pi$ stack with H36 and that of Q461 could hydrogen bond with V21 located in the neighboring subunit (Figure S1).[30] In addition, the CD spectra of pep9, pep9′, and pep7 showed that these structures were dominated by random coil (Figure S11B), perhaps because they were too short to fold into a full α-helix, which might be one of the main reasons for the loss of inhibition of L1-p formation.

The scrambled pep14 existed in a random coil and displayed no inhibition on L1-p formation (Figure S7B), illustrating the peptide sequence is critically important for inhibition. In addition, albeit the monosite mutants of pep14L459S and pep14F462S could fold into a partial α-helix (Figure S12A), they lost part of their capacity to inhibit L1-p formation (Figure S12B), illustrating that these two hydrophobic sites are critical for the competitive binding to L1 monomer.

Furthermore, pep14 showed inhibition not only on HPV 16 L1-p formation but also on that of HPV 58 L1 (Figure 4A). It is

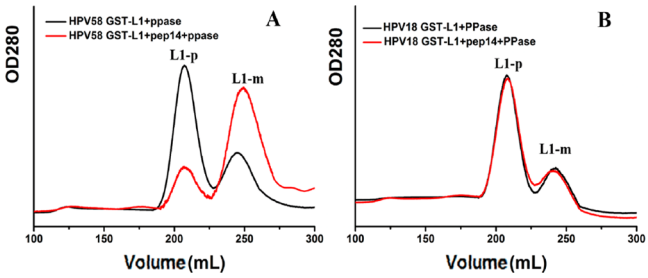

Figure 4. FPLC elution profiles of (A) HPV 58 L1 and (B) HPV 18 L1 before and after pretreatment by pep14. GST-L1 (1.25 nM) was incubated with peptides at a molar ratio of 1:100 in buffer L.

critically important since one of the great challenges of the current prophylactic HPV vaccine is its highly type-specific protection, that is, one subtype of VLP vaccine can prevent the infections only by its specific target. Therefore, the present study will serve to broaden the spectrum of peptide drugs in future antivirus agents, as pep14 originated from 16 L1 and was designed especially to target 16 L1. However, pep14 cannot inhibit the L1-p formation of HPV 18 (Figure 4B), which might be attributed to the fact that the two subtypes (HPV16/58) possess higher conservation than that between HPV 18 and 16 (Figure S13) in the target segment. Further improvements are needed to expand the broad-spectrum of peptide inhibitors.

DOI: 10.1021/ml500392y
ACS Med. Chem. Lett. 2015, 6, 381−385

In summary, the designed peptides demonstrated competitive binding with the L1 monomer and subsequently inhibited the formation of L1 pentamer. The length, sequence, and corrected folding of the peptide are critical factors for its inhibition of L1 pentamer formation. In addition, the hydrophobic residues of L459 and F462 proved to play a key role in the peptide function. The GST-released L1 could form L1 pentamers and VLPs readily after the peptide was removed from the system by dialysis, illustrating clearly the reversibility of the inhibition. Especially, pep14 targeting HPV 16 L1 could inhibit the formation of pentamer in other subtypes such as 58 L1. These findings lay the groundwork for the development of cost-effective, broad-spectrum peptide inhibitors to prevent HPV L1 pentamer and/or VLPs assembly, emerging as a new series of prophylactic and/or therapeutic agents for HPV. Hopefully, similar protocols could be extended to the treatment of other kinds of viruses.

■ ASSOCIATED CONTENT

Supporting Information

Experimental procedures; structural analysis on protein; plots of S_p/S_m; FPLC elution profiles of control peptides on L1-p formation; FRET assay on pep14-Scr and GST-L1, and pep14 and GST tag interactions; DLS, TEM of particle sizes; and CD spectra of peptides. This material is available free of charge via the Internet at http://pubs.acs.org.

■ AUTHOR INFORMATION

Corresponding Author

*Fax: +86-431-85193421. Tel: +86-431-85168730. E-mail: yqwu@jlu.edu.cn.

Author Contributions

The manuscript was written through contributions of all authors. All authors have given approval to the final version of the manuscript.

Notes

The authors declare no competing financial interest.

■ ACKNOWLEDGMENTS

The present work was supported by the NSFC (Nos. 21373101, 91027027 and 20934002) and the Innovation Program of State Key Laboratory for Supramolecular Structure and Materials.

■ ABBREVIATIONS

HPVs, Human papillomaviruses; VLPs, virus-like particles; GST, glutathione S-transferase; L1-p, L1 pentamer; L1-m, L1 monomer; SEC, size-exclusion chromatography; PPase, PreScissionTM Protease; FPLC, fast protein liquid chromatography

■ REFERENCES

(1) Hebner, C. M.; Laimins, L. A. Human papillomaviruses: basic mechanisms of pathogenesis and oncogenicity. *Rev. Med. Virol.* **2006**, *16*, 83−97.

(2) Hanslip, S. J.; Zaccai, N. R.; Middelberg, A. P. J.; Falconer, R. J. Assembly of human papillomavirus type-16 virus-like particles: multifactorial study of assembly and competing aggregation. *Biotechnol. Prog.* **2006**, *22*, 554−560.

(3) Walboomers, J. M. M.; Jacobs, M. V.; Manos, M. M.; Bosch, F. X.; Kummer, J. A.; Shah, K. V.; Snijders, P. J. F.; Peto, J.; Meijer, C.; Munoz, N. Human papillomavirus is a necessary cause of invasive cervical cancer worldwide. *J. Pathol.* **1999**, *189*, 12−19.

(4) Das, B. C.; Gopalkrishna, V.; Hedau, S.; Katiyar, S. Cancer of the uterine cervix and human papillomavirus infection. *Curr. Sci. India* **2000**, *78*, 52−63.

(5) Giroglou, T.; Flroin, L.; Schäfer, F.; Streeck, R. E.; Sapp, M. Human papillomavirus infection requires cell surface heparin sulfate. *J. Virol.* **2001**, *75* (3), 1565−1570.

(6) Culp, T. D.; Budgeon, L. R.; Christensen, N. D. Human papillomaviruses bind a basal extracellular matrix component secreted by keratinocytes which is distinct from a membrane-associated receptor. *Virology* **2006**, *374*, 147−159.

(7) Buck, C. B.; Day, P. M.; Trus, B. L. The papillomavirus major capsid protein L1. *Virology* **2013**, 169−174.

(8) Kines, R. C.; Thompson, C. D.; Lowy, D. R.; Schiller, J. T.; Day, P. M. The initial steps leading to papillomavirus infection occur on the basement membrane prior to cell surface binding. *Proc. Natl. Acad. Sci. U.S.A.* **2009**, *106*, 20458−20463.

(9) Day, P. M.; Baker, C. C.; Lowy, D. R.; Schiller, J. T. Establishment of papillomavirus infection is enhanced by promyelocytic leukemia protein (PML) expression. *Proc. Natl. Acad. Sci. U.S.A.* **2004**, *101*, 14252−14257.

(10) Day, P. M.; Gambhira, R.; Roden, R. B. S.; Lowy, D. R.; Schiller, J. T. Mechanisms of human papillomavirus type 16 neutralization by L2 cross-neutralizing and L1 type-specific antibodies. *J. Virol.* **2008**, *82*, 4638−4646.

(11) Pomfret, T. C.; Gagnon, J. M., Jr; Gilchrist, A. T. Quadrivalent human papillomavirus (HPV) vaccine: a review of safety, efficacy, and pharmacoeconomics. *J. Clin. Pharm. Ther.* **2011**, *36*, 1−9.

(12) Brisson, M.; Velde, N. V.; Wals, P. D.; Boily, M. C. The potential cost-effectiveness of prophylactic human papillomavirus vaccines in Canada. *Vaccine* **2007**, *25*, 5399−5408.

(13) Kemp, T. J.; Hildesheim, A.; Safaeian, M.; Dauner, J. G.; Pan, Y.; Porras, C.; Schiller, J. T.; Lowy, D. R.; Herrero, R.; Pinto, L. A. HPV16/18L1 VLP vaccine induces cross-neutralizing antibodies that may mediate cross-protection. *Vaccine* **2011**, *29*, 2011−2014.

(14) Steinbrook, R. The potential of human papillomavirus vaccines. *N. Engl. J. Med.* **2006**, *354*, 1109−1112.

(15) Buck, C. B.; Thompson, C. D.; Roberts, J. N.; Müller, M.; Lowy, D. R.; Schiller, J. T. Carrageenan is a potent inhibitor of papillomavirus infection. *PLoS Pathog.* **2006**, *2*, e69.

(16) Luciani, S.; Jauregui, B.; Kieny, C.; Andrus, J. K. Human papillomavirus vaccines: new tools for accelerating cervical cancer prevention in developing countries. *Immunotherapy* **2009**, *1*, 795−807.

(17) Wilson, A. J. Inhibition of protein-protein interactions using designed molecules. *Chem. Soc. Rev.* **2009**, *38*, 3289−3300.

(18) Sticht, J.; Humbert, M.; Findlow, S.; Bodem, J.; Müller, B.; Dietrich, U.; Werner, J.; Kr äusslich, H. G. A peptide inhibitor of HIV-1 assembly in vitro. *Nat. Struct. Mol. Biol.* **2005**, *12*, 671−677.

(19) Kulkarni, S. S.; Hu, X.; Doi, K.; Wang, H. G.; Manetsch, R. Screening of protein-protein interaction modulators via sulfo-click kinetic target-guided synthesis. *ACS Chem. Biol.* **2011**, *6*, 724−732.

(20) Stigers, K. D.; Soth, M. J.; Nowick, J. S. Designed molecules that fold to mimic protein secondary structures. *Curr. Opin. Chem. Biol.* **1999**, *3*, 714−723.

(21) Hu, X.; Manetsch, R. Kinetic target-guided synthesis. *Chem. Soc. Rev.* **2010**, *39*, 1316−1324.

(22) Mercer, D. K.; O'Neil, D. A. Peptides as the next generation of anti-infectives. *Future Med. Chem.* **2013**, *5*, 315−337.

(23) Conway, M. J.; Meyers, C. Replication and assembly of human papillomaviruses. *J. Dent. Res.* **2009**, *88*, 307−317.

(24) Baker, T. S.; Newcomb, W. W.; Olson, N. H.; Cowsert, L. M.; Olson, C.; Brown, J. C. Structures of bovine and human papillomaviruses. Analysis by cryoelectron microscopy and three-dimensional image reconstruction. *Biophys. J.* **1991**, *60*, 1445−1456.

(25) Bishop, B.; Dasgupta, J.; Chen, X. S. Structure-based engineering of papillomavirus major capsid L1: controlling particle assembly. *Virol. J.* **2007**, *4*, 3.

(26) Chen, X. S.; Casini, G.; Harrison, S. C.; Garcea, R. L. Papillomavirus capsid protein expression in Escherichia coli:

DOI: 10.1021/ml500392y
ACS Med. Chem. Lett. 2015, 6, 381−385

purification and assembly of HPV11 and HPV16L1. *J. Mol. Biol.* **2001**, *307*, 173−182.
(27) Zheng, D. D.; Fu, D. Y.; Wu, Y.; Sun, Y. L.; Tan, L.-L.; Zhou, T.; Ma, S.-Q.; Yang, Y.-W. Efficient inhibition of human papillomavirus 16 L1 pentamer formation by a carboxylatopillarene and a p-sulfonatocalixarene. *Chem. Commun.* **2014**, *50*, 3201−3203.
(28) Zheng, D. D.; Pan, D.; Zha, X.; Wu, Y.; Jiang, C.; Yu, X. In vitro monitoring of the formation of pentamers from the monomer of GST-L1 fused HPV 16L1. *Chem. Commun.* **2013**, *49*, 8546−8548.
(29) Jin, S.; Pan, D.; Yu, X.; Wu, Y.; Liu, Y.; Yin, F.; Chen, X. S. The critical residues of helix 5 for in vitro pentamer formation and stability of the papillomavirus capsid protein, L1. *Mol. BioSyst.* **2014**, *10*, 724−727.
(30) Bishop, B.; Dasgupta, J.; Klein, M.; Garcea, R. L.; Christensen, N. D.; Zhao, R.; Chen, X. S. Crystal strctures of four types of human papillomavirus L1 capsid proteins. *J. Biol. Chem.* **2007**, *282*, 31803−31811.
(31) Song, Y.; Rodgers, V. G. J.; Schultz, J. S.; Liao, J. Protein interaction affinity determination by quantitative FRET technology. *Biotechnol. Bioeng.* **2012**, *109*, 2875−2883.
(32) Yan, C.; Yang, B.; Yu, Z. Determination of silk fibroin secondary structure by terahertz time domain spectroscopy. *Anal. Methods* **2014**, *6*, 248−252.

DOI: 10.1021/ml500392y
ACS Med. Chem. Lett. 2015, 6, 381−385